Pergamon PII: S0016-0032(97)00073-2

J. Franklin Inst. Vol. 335B, No. 7, pp. 1283–1297, 1998

Published by Elsevier Science Ltd
Printed in Great Britain
0016-0032/98 $19.00+0.00

Generation of Current Conveyor Based Lowpass Filters from a Passive RLC Filter

by AHMED M. SOLIMAN*

Electronics and Communication Engineering Department, Cairo University, Cairo, Egypt

(Received in final form 27 April 1997; accepted 23 July 1997)

ABSTRACT: *It is shown that three recently reported current conveyor based lowpass filters are originated from a passive RLC filter. Two new grounded-capacitor current mode lowpass filters are also introduced. Frequency limitation equations based on the non-ideal current conveyors are given. PSpice simulation results are included.* © 1998 The Franklin Institute. Published by Elsevier Science Ltd

I. Introduction

Passive RLC filters remain as the starting origin of low sensitivity active filters, regardless of the active element used. Due to the finite gain bandwidth of the operational amplifier (op amp) (**1**), the current conveyor (CCII) (**2**) is now used as the active element, in several recently reported filters. Most of the CCII filters introduced in the literature are generated from the conventional op amp filters using the adjoint network theorem (**3**), or using the transformation theorem relating a class of op amp to CCII circuits (**4**) or using the nullor equivalent circuit approach (**5**). In all these methods the generated CCII filter is equivalent to the original op amp filter only if both active devices are ideal. Similarly, in generating a CCII based filter circuit from another CCII filter circuit, they will only be equivalent under the assumption of ideal CCIIs.

In this paper, it is shown that the grounded-capacitor second-order non-inverting lowpass filter based on the well-known FDNR-C circuit (**6**) leads to the generation of other recently reported lowpass filters. Two new grounded-capacitor current mode lowpass filters are also introduced. Frequency limitation equations based on the non-ideal current conveyors are given. PSpice simulation results showing the magnitude characteristics of the theoretically equivalent family of lowpass filters are given.

II. The FDNR-C Based Lowpass Filter

The CC II filters considered in this paper are based on the passive RLC lowpass filter shown in Fig. 1(a), which is transformed to the active circuit shown in Fig. 1(b), using Bruton's transformation (**1**). Figure 2 represents the well-known CCII circuit (**6**)

* E-mail: asoliman@alpha1-eng.cairo.eun.eg.

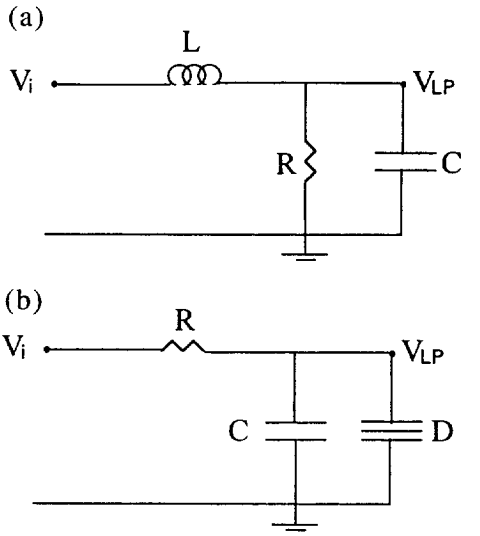

FIG. 1. (a) The passive RLC lowpass filter. (b) The lowpass filter based on Bruton's transformation.

which realizes either a parallel L-R circuit or a parallel FDNR-C circuit according to the proper selection of the admittances Y_1, Y_2 and Y_3. As stated in (**6**) the simulated FDNR-C circuit is very practical in realizing generalized lowpass filters; in particular, a second-order lowpass filter is realized as shown in Fig. 3(a) by connecting a resistor in series with this FDNR-C circuit in accordance with Fig. 1(b).

Assuming an ideal CCII−, the voltage transfer function of this grounded-capacitor non-inverting lowpass filter, is given by

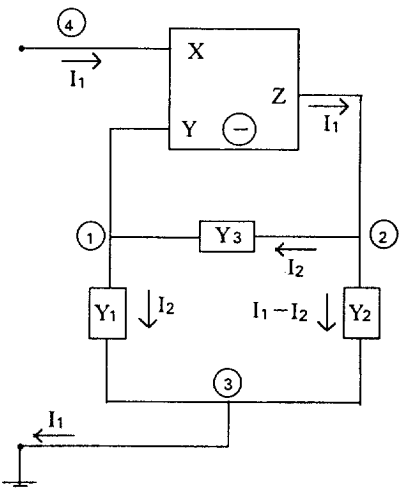

FIG. 2. The parallel L-R or FDNR-C circuit (**6**).

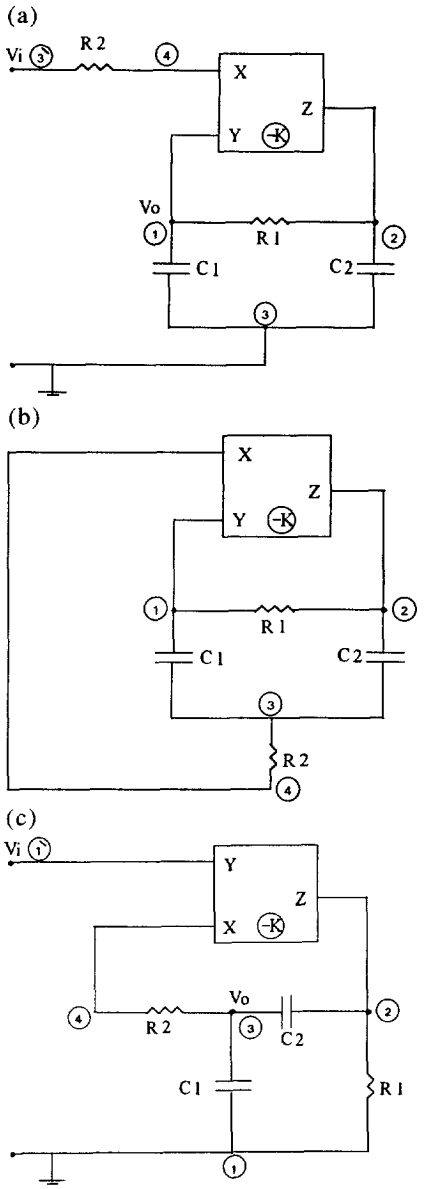

FIG. 3. (a) The grounded-capacitor second order lowpass filter (**6**). (b) The dead network obtained from Fig. 3(a). (c) The high input impedance lowpass filter (**8**).

$$T_v(S) \equiv \frac{V_0}{V_i} = \frac{1}{s^2 C_1 C_2 R_1 R_2 + s(C_1 + C_2)R_2 + 1}. \tag{1}$$

For a specified ω_0 and Q, the design equations are given by

$$C_1 = C_2 = C, \tag{2}$$

$$R_1 = \frac{2Q}{\omega_0 C}, \quad R_2 = \frac{1}{2Q\omega_0 C}. \tag{3}$$

The ω_0 and the Q passive sensitivities are given by

$$S_{R_1}^{\omega_0} = S_{R_2}^{\omega_0} = S_{C_1}^{\omega_0} = S_{C_2}^{\omega_0} = -\frac{1}{2}, \tag{4}$$

$$S_{R_1}^{Q} = -S_{R_2}^{Q} = \frac{1}{2}, \quad S_{C_1}^{Q} = -S_{C_2}^{Q} = -\frac{1}{2} + \frac{C_2}{C_1 + C_2}. \tag{5}$$

For the equal C design, the Q sensitivities with respect to C_1 and C_2 are equal to zero.

The lowpass filter shown in Fig. 3(a) can lead to the generation of two voltage mode and one current mode recently reported lowpass filters, as well as to two new grounded-capacitor current mode lowpass filters as will be explained in the following section. The capabilities of the circuit of Fig. 3(a) lies in the fact that the CCII employed is a CCII− and has infinite input impedance at node Y. Thus the current leaving node 3 is the same as the current entering the CCII at node 4 as demonstrated in Fig. 2. In other words node 3 can be floating (**6, 7**).

III. Generation Method

Setting V_i equal to zero in the circuit of Fig. 3(a) and removing the ground from node 3, the circuit of Fig. 3(b) is obtained, which has the same characteristic equation as given by the denominator of Eq (1). This dead circuit can be excited either by a voltage source or a current source according to the desirable mode of operation.

3.1. *Voltage mode filters*

Injecting the input voltage at the Y terminal of the CCII (node 1′) and connecting node 1 to ground, the circuit shown in Fig. 3(c) (**8**) is obtained which in the ideal case has the same lowpass transfer function as given by Eq (1). As a non-inverting lowpass filter however the circuit of Fig. 3(a) has the advantages over the circuit of Fig. 3(c) in using grounded capacitors, and in having better frequency characteristics as will be illustrated in Section 4.

The high input impedance lowpass filter reported in (**9**) can also be generated from the lowpass filter of Fig. 3(a) as explained next. Figure 4(a) represents a modified version of the circuit of Fig. 3(a) by adding a second CCII at the input to act as a voltage follower. Although the polarity of this CCII does not affect the operation of this circuit, it is taken as a CCII+ in order to demonstrate how the circuit of Fig. 4(b) can be generated from Fig. 4(a). Assuming ideal CCIIs it is seen that the current I which leaves Z_1 to node 2 in Fig. 4(a) is the same as the current which leaves Z_2 to ground. Thus by disconnecting Z_1 from node 2 (and grounding Z_1) and removing the ground from Z_2, and connecting Z_2 to node 2 to supply the same current I to the passive circuit, the circuit of Fig. 4(b) is obtained (**9**). In this case, $-K_1$ can be changed to K_1, that is, a CCII+ can be used instead of the CCII−, without affecting the circuit performance.

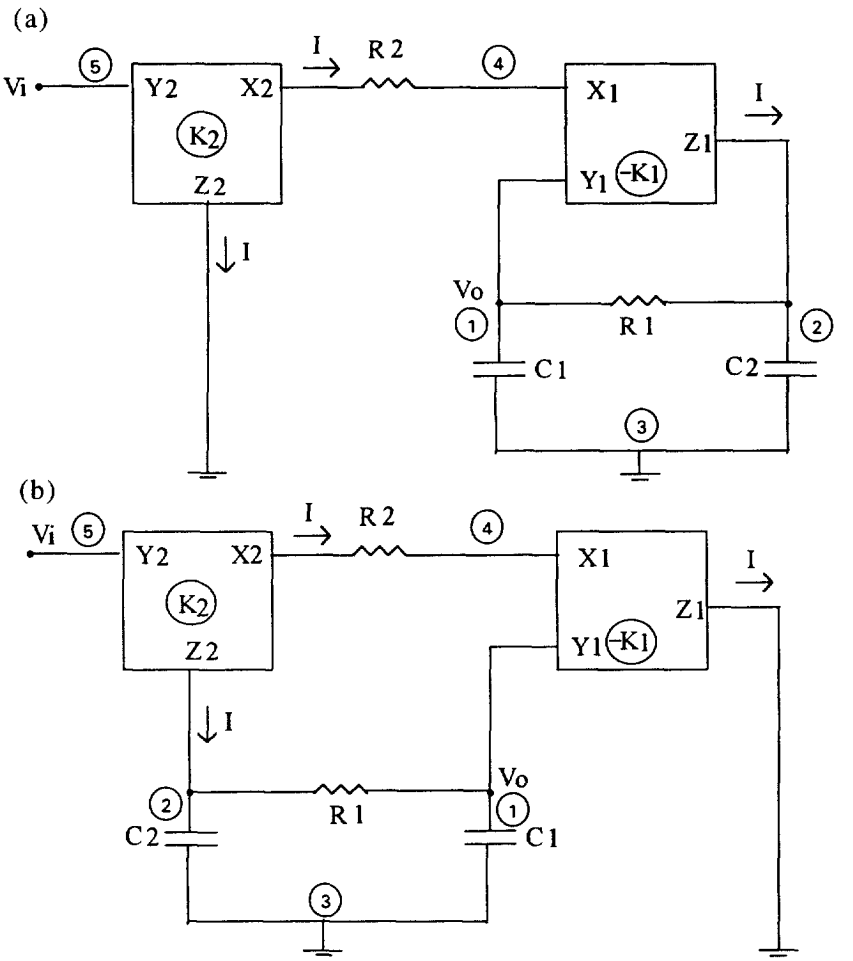

FIG. 4. The high input impedance grounded-capacitor lowpass filters.

3.2. *Current mode filters*

Three current mode lowpass filter circuits are given in this subsection, all of them having the same expression of the current transfer function as given by Eq (1), under the assumption of ideal CCIIs.

Figure 5(a) and (b) represent two new grounded-capacitor current mode lowpass filters. These two proposed circuits are generated from the circuit of Fig. 3(b) by applying the input current to node 2 and grounding node 3. In order to utilize the current flowing in R_2 which has a lowpass nature, a second CCII acting as a current follower is added to the circuit as shown in Fig. 5(a), or a two-output CCII is used as shown in Fig. 5(b).

The current-mode lowpass filter shown in Fig. 5(c) (**10**) can also be generated from the circuit of Fig. 3(b) by applying the input current to node 3 and grounding node 2.

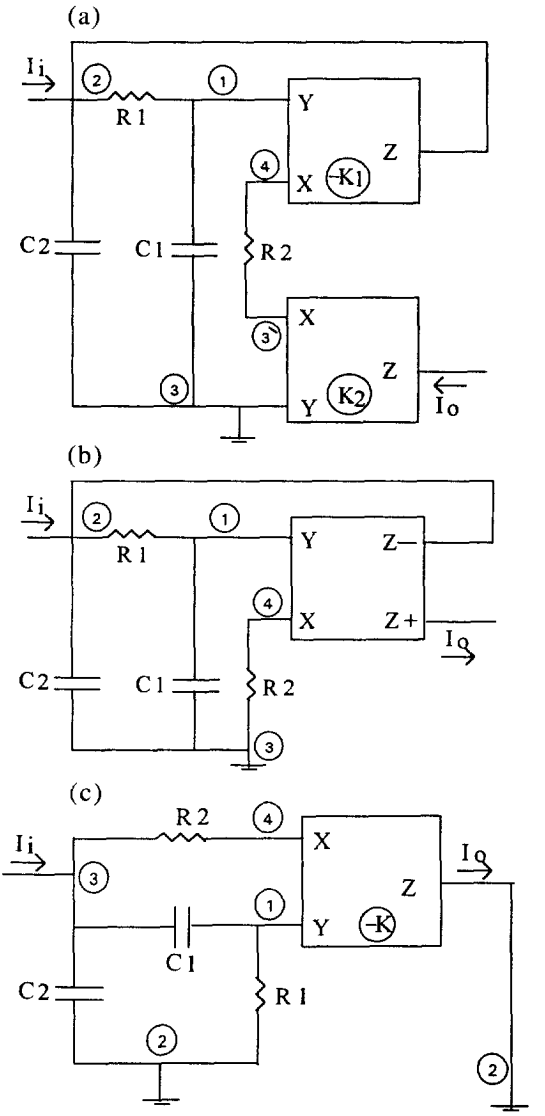

FIG. 5. (a) The new grounded-capacitor current mode lowpass filter using two CCII. (b) The new grounded-capacitor current mode lowpass filter using a two-output CCII. (c) The current mode lowpass filter (**10**).

IV. Effects of Non-ideal CCII

Assuming ideal CCII, the four voltage-mode and the three current-mode lowpass filters considered in this paper have the same transfer function. Practically however, their characteristics are different due to the non-ideal CCII. In this section, the effects

of the parasitic parameters, and the high frequency characteristics of the CCII are considered.

4.1. *Effect of R_x, R_z and C_z*

It is well known that the parasitic parameters of the CCII are R_x, R_z and C_z. Examining the circuits considered in this paper, it is seen that all the grounded capacitor circuits can absorb the effect of C_z by subtracting its value from C_2. On the other hand, they cannot absorb the effect of R_z. The circuit of Fig. 3(c) however can absorb the effect of R_z but it cannot absorb the effect of C_z. The effects of C_z and R_z however can be minimized by proper selection of the filter circuit components. The dominant parasitic parameter however which affects the filter characteristics is R_x. In order to compensate the effect of R_x, the design equation for R_2 should be modified to

$$R_2 = \frac{1}{2Q\omega_0 C} - aR_x, \tag{6}$$

where $a = 1$, for the circuits of Fig. 3(a) and (c) and Fig. 5(b) and (c), and $a = 2$, for the circuits of Fig. 4(a) and (b), and Fig. 5(a).

4.2. *Frequency limitation equations*

At high frequencies, the single output and the two-output CCII are described by the matrix equations

$$\begin{bmatrix} V_x \\ I_y \\ I_z \end{bmatrix} = \begin{bmatrix} 0 & B & 0 \\ 0 & 0 & 0 \\ \pm K & 0 & 0 \end{bmatrix} \begin{bmatrix} I_x \\ V_y \\ V_z \end{bmatrix}, \tag{7}$$

$$\begin{bmatrix} V_x \\ I_y \\ I_{z_1} \\ I_{z_2} \end{bmatrix} = \begin{bmatrix} 0 & B & 0 & 0 \\ 0 & 0 & 0 & 0 \\ -K & 0 & 0 & 0 \\ K & 0 & 0 & 0 \end{bmatrix} \begin{bmatrix} I_x \\ V_y \\ V_{z_1} \\ V_{z_2} \end{bmatrix}. \tag{8}$$

In the ideal case $K = B = 1$; practically however K and B are frequency dependent and are represented by the equations

$$K(s) = \frac{K_0}{1 + s/\omega_1}, \tag{9}$$

$$B(s) = \frac{B_0}{1 + s/\omega_2}, \tag{10}$$

where K_0 and B_0 are the DC values of $K(s)$ and $B(s)$, and they have magnitudes very close to one; ω_1 and ω_2 are the 3 dB radian frequencies of $K(s)$ and $B(s)$, respectively.

Taking K and B of the CCII as given by Eqs (9) and (10), the fractional shifts in ω_0 and Q of each of the filters considered in this paper can be calculated based on the Budak–Petrela method (**11, 12**). The transfer function and the fractional shifts in ω_0

TABLE I

Class	Circuit Fig.	Ref.	Transfer function	$\frac{\Delta\omega_0}{\omega_0}$	$\frac{\Delta Q}{Q}$
I	3(a)	(6)	$\frac{K}{s^2C_1C_2R_1R_2+s(C_1+C_2)R_2+KB}$	0	$\frac{\omega_0}{\omega_P}Q$
	4(a)	—	$\frac{K_1B_2}{s^2C_1C_2R_1R_2+s(C_1+C_2)R_2+K_1B_1}$	0	$\frac{\omega_0}{\omega_P}Q$
	4(b)	(9)	$\frac{K_2B_2}{s^2C_1C_2R_1R_2+s(C_1+C_2)R_2+K_2B_1}$	0	$\frac{\omega_0}{\omega_P}Q$
	5(a), 5(b)	—	$\frac{K_2B_1}{s^2C_1C_2R_1R_2+s(C_1+C_2)R_2+K_1B_1}$	0	$\frac{\omega_0}{\omega_P}Q$
II	3(c)	(8)	$\frac{B[1+sC_2R_1(1-K)]}{s^2C_1C_2R_1R_2+s[(C_1+C_2)R_2+C_2R_1(1-K)]+1}$	$-\frac{\omega_0}{\omega_1}Q$	$\frac{\omega_0}{\omega_1}Q$
	5(c)	(10)	$\frac{K[1+sC_1R_1(1-B)]}{s^2C_1C_2R_1R_2+s[(C_1+C_2)R_2+C_1R_1(1-B)]+1}$	$-\frac{\omega_0}{\omega_2}Q$	$\frac{\omega_0}{\omega_2}Q$

and Q of each of the lowpass filters considered are given in Table 1, where ω_P is defined by

$$\frac{1}{\omega_P}=\frac{1}{\omega_1}+\frac{1}{\omega_2}. \tag{11}$$

It is seen that the transfer functions of the circuits of Figs 3(a), 4 and 5(a) and (b) are of similar nature and are different from those of the circuits of Fig. 3(c) and Fig. 5(c).

The voltage-mode circuit of Fig. 3(c) (**8**) has $\Delta\omega_0$ and ΔQ that are dependent on the 3 dB frequency of $K(s)$. On the other hand the current-mode circuit of Fig. 5(c) (**10**) has similar expressions for $\Delta\omega_0$ and ΔQ to those of the circuit of Fig. 3(c) with ω_1 replaced by ω_2.

V. Simulation Results

PSpice simulations of the circuits considered in this paper are carried out using the AD844 A/AD biased with ± 9 V. The lowpass filter considered here has a maximally flat response with $f_0 = 1$ MHz, which is realizable taking $C_1 = C_2 = 0.1$ nF, $R_1 = 2.25\,\text{k}\Omega$ and $R_2 = 1.125\,\text{k}\Omega$.

The simulations included in this paper are based on the well-known realization of the CCII−, based on using two CCII+, with the second CCII+ acting as a current follower.

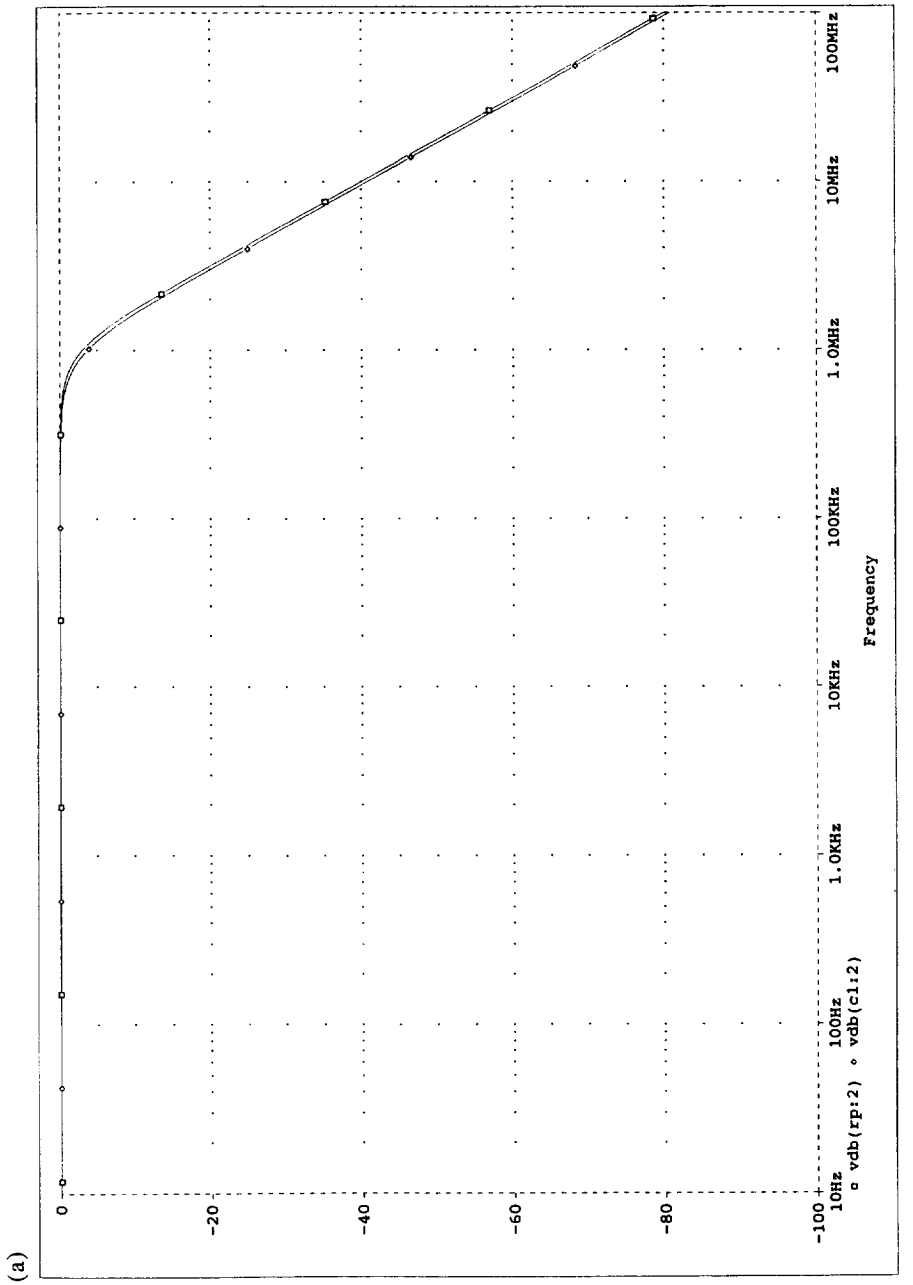

FIG. 6. (a) The magnitude characteristics of the lowpass filter of Fig. 3(a).

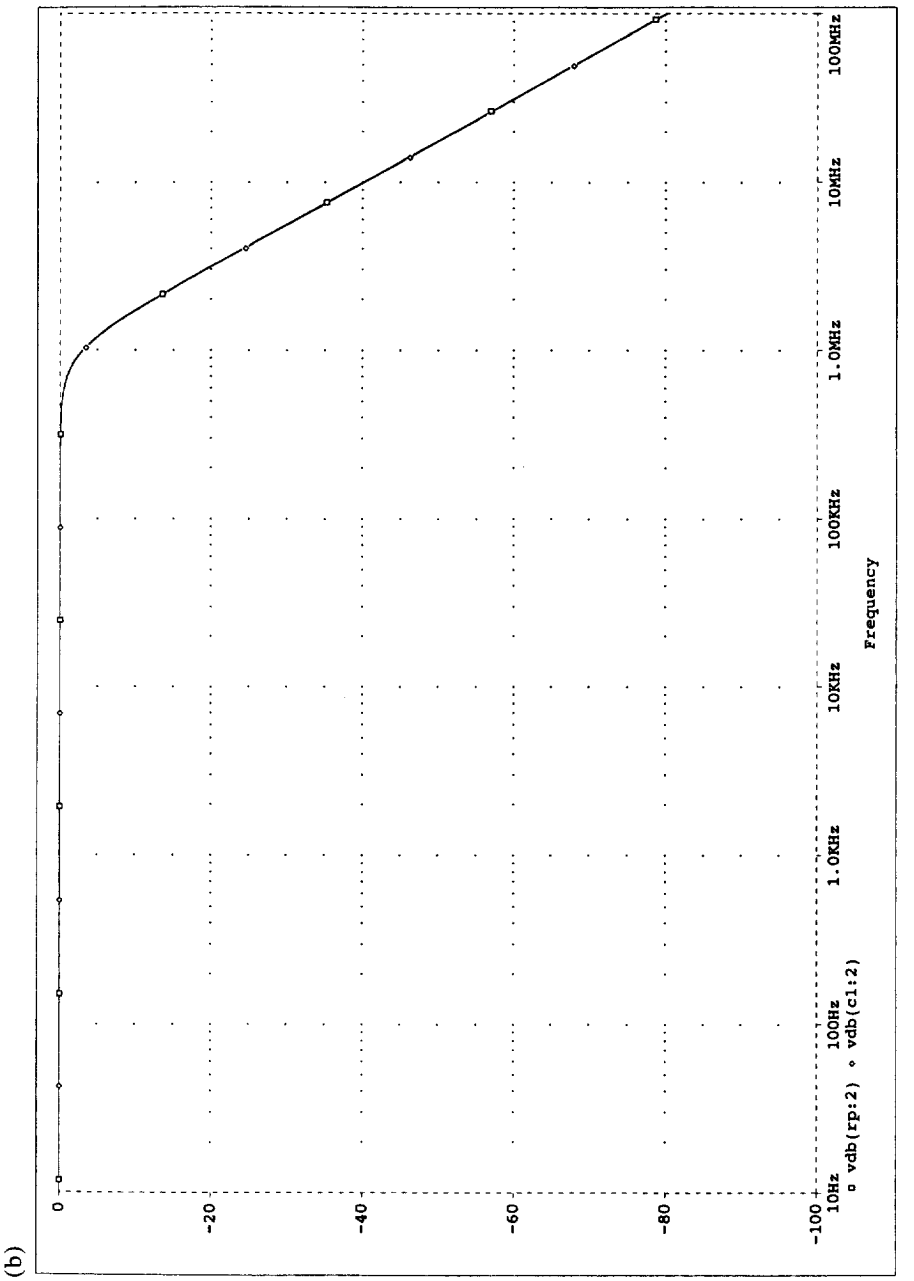

FIG. 6. (b) The magnitude characteristics of the compensated lowpass filter of Fig. 3(a).

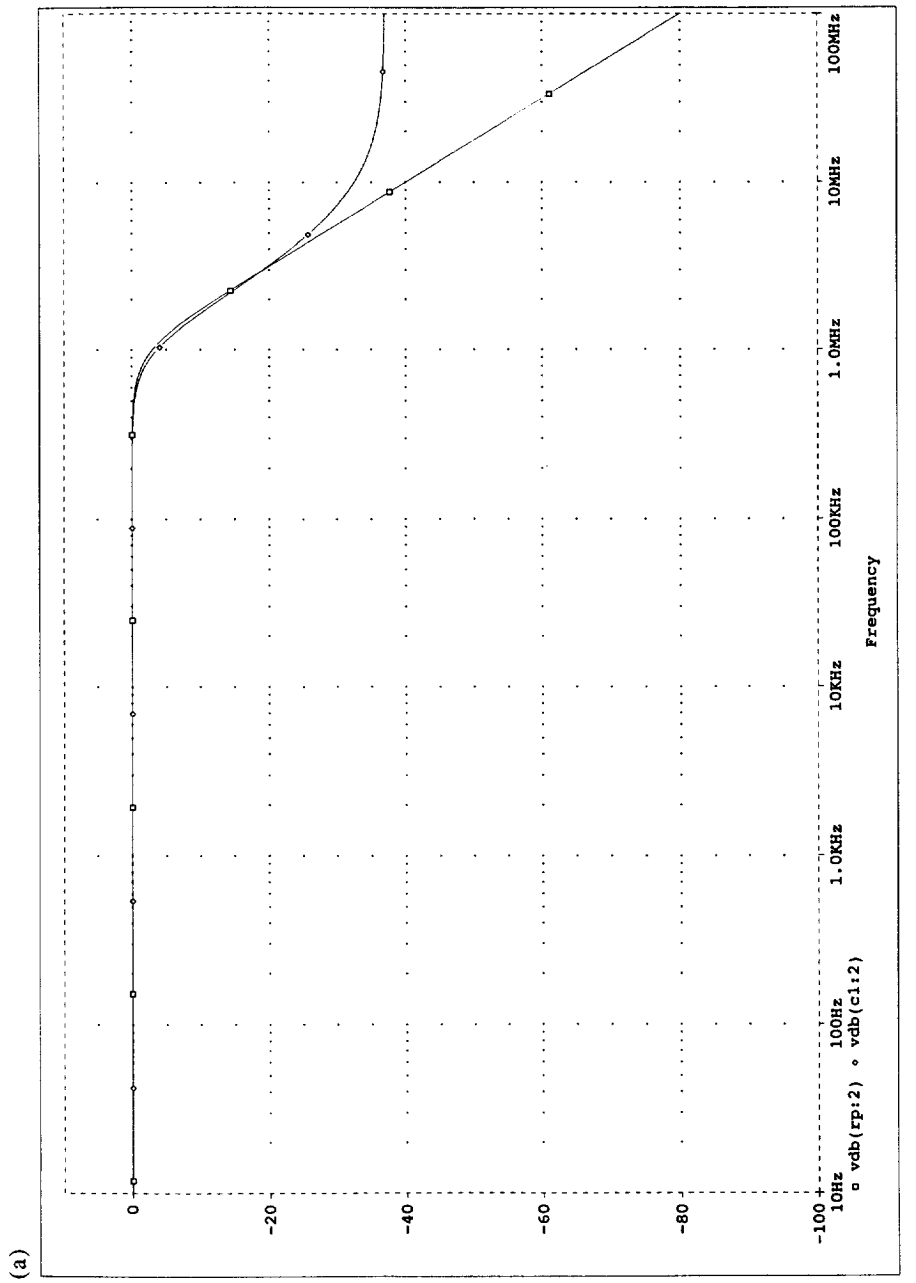

FIG. 7. (a) The magnitude characteristics of the lowpass filter of Fig. 3(c).

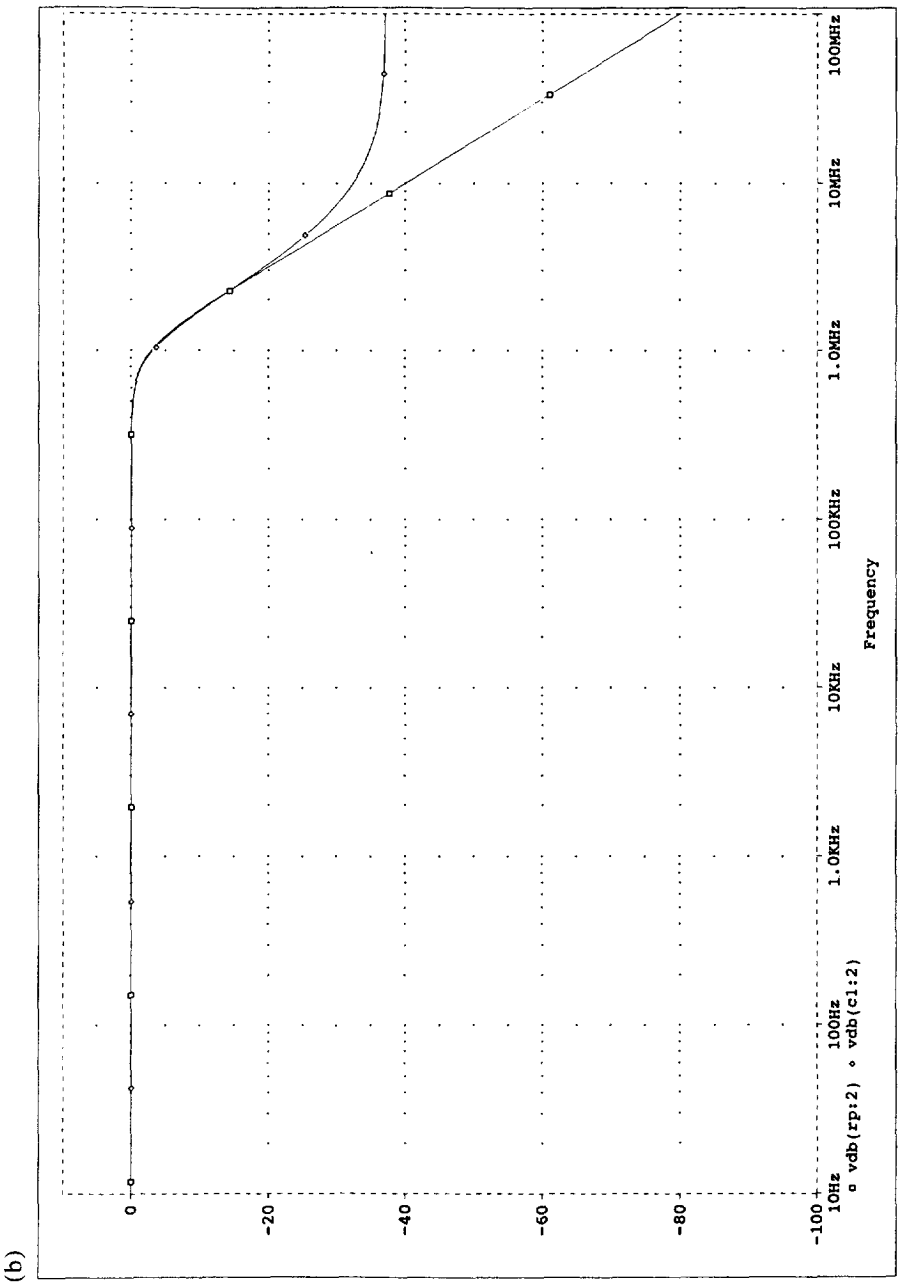

FIG. 7. (b) The magnitude characteristics of the compensated lowpass filter of Fig. 3(c).

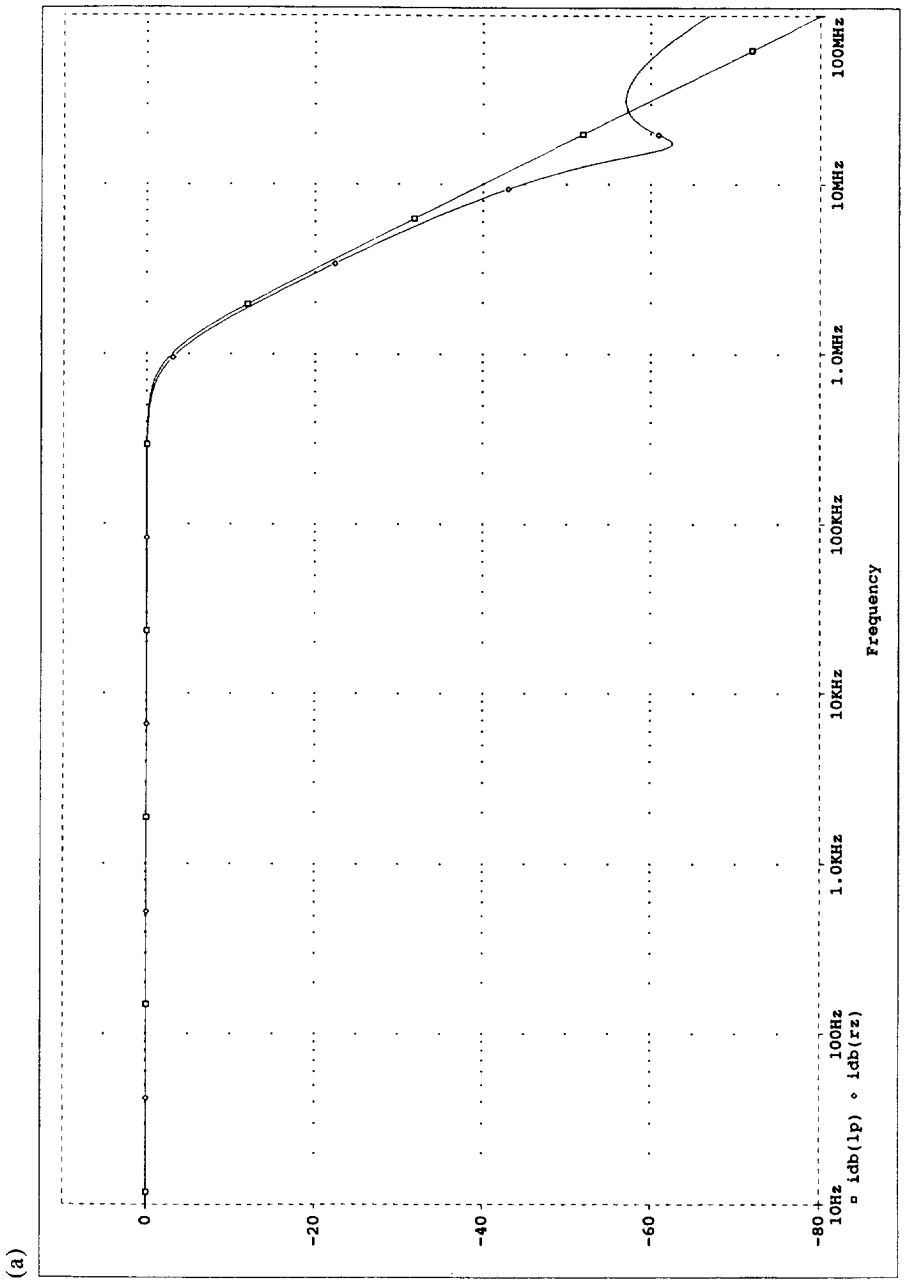

FIG. 8. (a) The magnitude characteristics of the lowpass filter of Fig. 5(c).

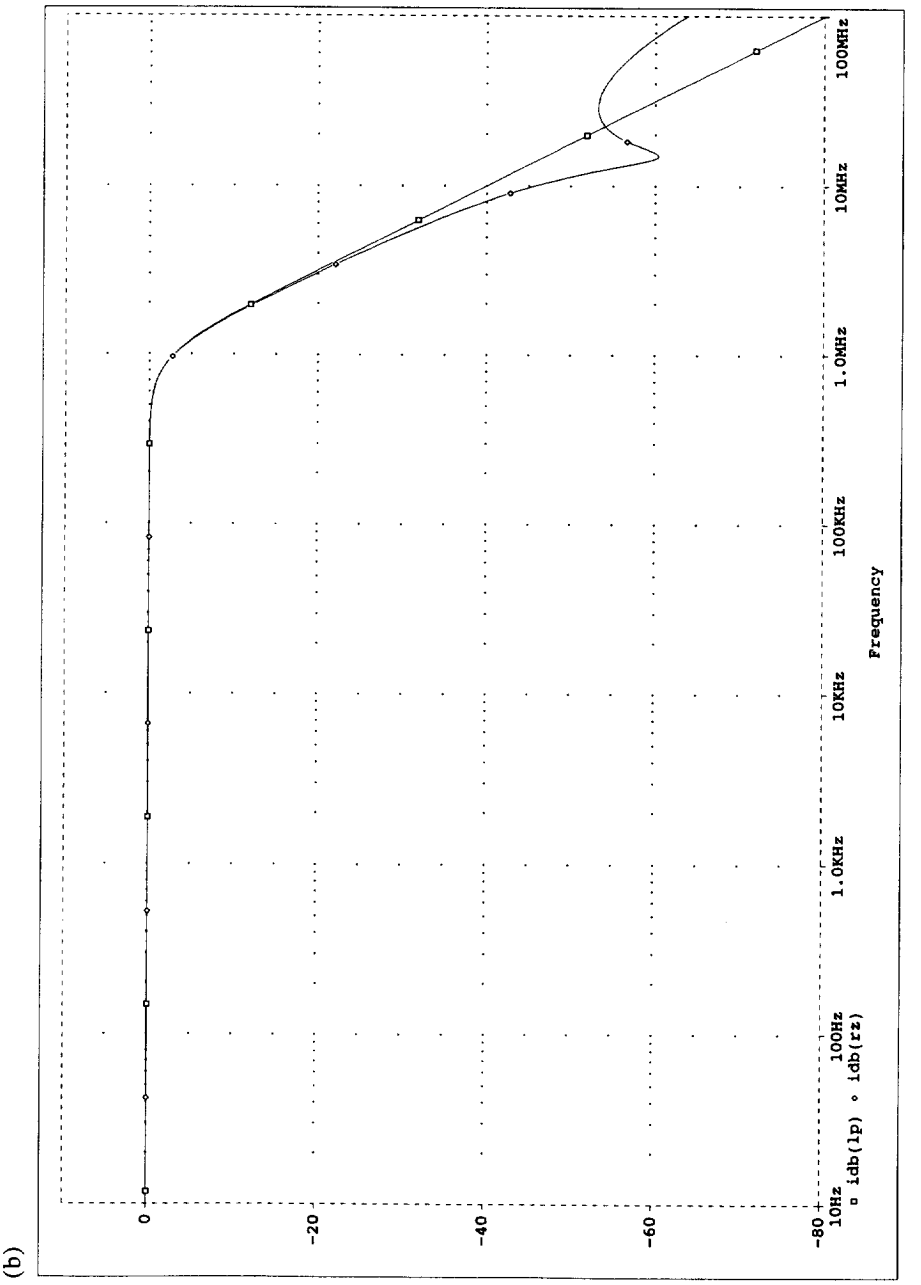

FIG. 8. (b) The magnitude characteristics of the compensated lowpass filter of Fig. 5(c).

Figure 6(a) represents the magnitude response of the circuit of Fig. 3(a) which is very close to the ideal response obtained from the passive RLC filter. It is seen that there is a very small error in ω_0 which is mainly due to R_x.

For the AD844 A/AD, $R_x = 65\,\Omega$, and its effect can be easily compensated as given by Eq (6). In this case, the magnitude characteristics coincide with the ideal response as shown in Fig. 6(b).

Figure 7(a) and (b) represent the simulation results of the circuit of Fig. 3(c) which indicate large magnitude error starting from 2 MHz.

The simulations of the circuit of Fig. 5(c) with a load resistance of 1 kΩ are given in Fig. 8 (a) and (b), which show a notch frequency at about 20 MHz; this is due to the error in the numerator of the transfer function which is dependent on the voltage tracking error function $B(s)$.

Conclusions

A family of CCII based lowpass filters are generated from the circuit of Fig. 3(a). It is found that the circuits can be classified in two classes: Class I which includes the circuits of Fig. 3(a), Fig. 4(a) and (b) and Fig. 5(a) and (b) and Class II includes the circuits of Fig. 3(c) and Fig. 5(c). It is found that the Class I circuits are superior to the Class II circuits since they employ grounded-capacitors and they have better high frequency characteristics as demonstrated by the simulations included.

References

(1) Huelsman, L. P., *Active and Passive Analog Filter Design*. McGraw-Hill, 1993.

(2) Sedra, A. and Smith, K. C., A second generation current conveyor and its applications. *IEEE Trans. Circuit Theory*, 1970, **17**, 132–134.

(3) Roberts, G. W. and Sedra, A. S., All current mode frequency selective circuits. *Electron. Lett.*, 1989, **25**, 759–761.

(4) Soliman, A. M., Theorem relating a class of op amp and CC II circuits. *Internat. J. Electron.*, 1995, **79**, 53–61.

(5) Svoboda, J. A., Current conveyors, operational amplifiers and nullors. *Proc. IEEG*, 1989, **136**, 317–322.

(6) Soliman, A. M., Ford-Girling equivalent circuit using CC II. *Electron. Lett.*, 1978, **14**, 721–722.

(7) Senani, R., Novel active RC circuit for floating inductor simulation. *Electron. Lett.*, 1979, **15**, 679–680.

(8) Liu, S. I. and Tsao, H. W., The single CC II biquads with high input impedance. *IEEE Trans. Circuits Syst.*, 1991, **38**, 456–461.

(9) Fabre, A., Dayoub, F., Duruisseau, I. and Kamoun, M., High input impedance insensitive second order filters implemented from current conveyors. *IEEE Trans. Circuits Syst.*, 1994, **41**, 918–921.

(10) Liu, S. I., Tsao, H. W. and Wu, J., Cascadable current-mode single CC II biquads. *Electron Lett.*, 1990, **26**, 2005–2006.

(11) Budak, A., *Passive and Active Network Analysis and Synthesis*. Houghton Mifflin, 1974.

(12) Awad, I. A., Abd-El Gawad, S. Y. and Soliman, A. M., Simplified formulas for $\Delta\omega_0/\omega_0$ and $\Delta Q/Q$ based on Budak–Petrela's method. *IEEE Trans. Circuits Syst.*, 1995, **42**, 186–187.